DOI: 10.48011/asba.v2i1.1277

ANALYSIS OF AN EOLIC-PHOTOVOLTAIC HYBRID GENERATION WITH SYNCHRONVERTER FOR FREQUENCY AND VOLTAGE SUPPORTS IN A MICROGRID

Maxwel da Silva Santos*, Luciano Sales Barros†, Rafael Lucas da Silva França*, Flavio Bezerra Costa*, Camila Mara Vital Barros†, Kai Strunz‡

* *Federal University of Rio Grande do Norte*
Natal, RN, Brazil

† *Federal University of Paraíba*
João Pessoa, PB, Brazil

‡ *Technische Universität Berlin*
Berlin, Germany

Emails: maxwel@ufrn.edu.br, lsalesbarros@ci.ufpb.br, rafaellucas@ufrn.edu.br, flaviocosta@ect.ufrn.br, camila.barros@ci.ufpb.br, kai.strunz@tu-berlin.de

Abstract— A microgrid consists of a grid able to operate in connection to the main interconnected power system or in island mode. This paper deals with a microgrid containing a small hydroelectric power plant (HPP), a battery energy storage system (BESS), a wind energy conversion system (WECS), and a photovoltaic array (PV). The WECS and PV systems are connected to the grid through one full-power voltage source converter (VSC). In order to provide frequency and voltage supports to the microgrid, the VSC is controlled by a virtual synchronous generator (VSG) technique of synchronverter. The considered scenario was divided into three parts: first, the microgrid operates connected to the main system and then it starts operating in island mode; posteriorly, frequency and voltage variations occur due to load variations in the microgrid; finally, the microgrid returns to operate connected to the interconected system. Simulation results have shown that the synchronverter is an alternative to provide efficient frequency and voltage control to a microgrid for both connected and island modes, considering a hybrid generation unit.

Keywords— eolic-photovoltaic hybrid distributed generation, full-power converter, microgrid, synchronverter, virtual synchronous generator.

1 Introduction

The microgrid concept has been proposed for an efficient and flexible utilization of distributed energy resources. The microgrid can be defined as a grid where interconnected loads and distributed energy resources act as a single controllable entity with respect to the interconnected system in order to operate in both grid connected or island modes. In that way, it provides a more flexible and reliable system. Besides that, the presence of distributed generation (DG) sources improves efficiency of the overall system (Meng et al., 2015). The microgrid ability to operate in island mode is subject to the existence of synchronous generation (SG), since SGs provide the energy balance in the microgrid.

The BESS and their integration to the power grid have become increasingly important, due to the perpetual load growth results in a stressed and less secure power system operation. In recent years, the capital cost of battery storage technologies has significantly reduced, thus justifying a new study of its applications and economic benefits (Mercier et al., 2009).

The electrical power system is currently undergoing a change from centralized generation to DGs. However, most of these comprise in DC sources, variable frequency sources or asynchronous frequency sources with the grid frequency. Therefore, they require converters to be connected to the grid (Zhong and Rohner, 2011). In eolic sources, the WECS applications with full power converters have been increasing since the converter allows the operation of the wind turbine in wide ranges of speed, allowing a more efficient captivation from the available wind power (Barros and Barros, 2017). Among the grid connected WECS that employ full power converters, the ones based on PMSG have wide range of speed, high power to weight ratio, high efficiency, and do not require external excitation (Barros and Barros, 2017). Regarding solar sources, the PV energy has experienced a remarkable growth for the past two decades in its widespread use from stand alone to utility interactive PV systems (Villalva et al., 2009). A PV system directly converts sunlight into electrical energy. However, the obtained energy depends on solar radiation, temperature, and the voltage or current produced in the photovoltaic module (Villalva et al., 2009).

The current paradigm in the generation control of WECS or PV is to extract the maximum power from the source and to inject it into the power grid. However, with the significant growth of renewable power sources, the traditional method for injecting all available power to the grid may become untenable (Zhong and Rohner, 2011). Therefore, it is necessary to operate renewable sources in the same way as conventional SGs or at least to mimic certain aspects of the operation. Thus, synchronverter-based VSG concept proposed in (Zhong and Rohner, 2011) has been emerged.

This paper provide a performance analysis in terms of frequency and voltage support of the eolic-photovoltaic hybrid generation connected to the microgrid using a VSC controlled by the synchronverter technique with the goal to maintaining the stability of the grid. The microgrid is connected to the interconnected system or in island mode with load variations. Dynamic models of HPP, wind turbine with PMSG, PV, BESS, interfacing converters and their controls, and power grid have been implemented. The integration of these models in simulation environment has been carried out, constituting a platform of simulation of microgrid with DG sources and energy storage system (ESS).

This paper is organized according to the following structure: in Section 2, the HPP, WECS, PV, and BESS models are presented. In Section 3, the synchronverter model and control strategy are presented. Section 4 presents simulation results and their analysis. At the end, the conclusions are presented.

2 Grid and Distributed Generation Models and Controls

This section defines the grid and distributed generation models as well as their control systems. The interconnected system is represented by a three-phase ideal AC source connected to a microgrid by an islanding circuit breaker (ICB). The used line model is the π-nominal. The used load model is the constant impedance. All the used transformers model is the delta–grounded wye step-down connection. The models implemented in this paper can be found in (Kersting., 2002).

2.1 Hydroelectric Power Plant Model

Fig. 1 depicts the HPP model with a speed regulator. Table 1 summarizes the HPP parameters.

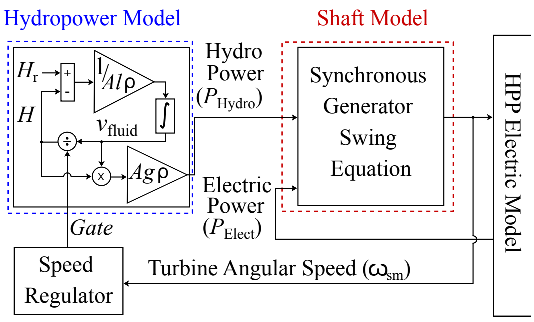

Figure 1: HPP model with speed regulator.

The hydraulic turbine considered in this paper is of the fixed blade type. The dynamic model of the turbine was presented in (Kundur, 1994). The velocity of fluid V_{fluid} in the duct upon reaching at the turbine and the power captured by the hydraulics turbine P_{hydro} are given by:

$$V_{fluid} = \frac{1}{Al\rho} \int (H_r - H) \tag{1}$$

and

$$P_{Hydro} = A\rho g (V_{fluid} H), \tag{2}$$

where H_r is the rated height of the water column, H is the height of the water column, A is the cross section area of the duct, l is the duct length, ρ is the density of water and g is the gravity acceleration.

The governor is the extracted power control system, so it sets the proper gate opening depending on the desired turbine speed.

The used synchronous machine model is the classic one with constant field voltage and equivalent circuit with internal voltage behind transient reactance (Kundur, 1994). In this model, only the angle of internal voltage varies according to the required electrical power of the machine according to:

$$\frac{d\,\omega_{sm}}{dt} = \frac{1}{J_{sm} 2\pi f}(P_{Hydro} - P_{Elect}), \tag{3}$$

where J_{sm} is the inertia of the set and P_{elect} is the supplied electric power.

Table 1: HPP Parameters.

Parameters	Value	Unit
P	30	MW
V	13.8	KV
H_r	75	m
V_{fluid}	4	m/s
A	10	m^2
l	25	m
ρ	1000	Kg/m^3
J_{sm}	7036	Kg/m^2
X_{sm}	30	mH

2.2 PMSG-Based Wind Energy Generator Model

Fig. 2 depicts the WECS model, which consists of three parts, the aerodynamic model, the shaft model, and the PMSG electric model. Table 2 summarizes the PMSG parameters.

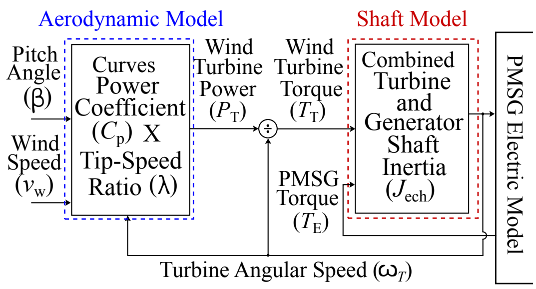

Figure 2: WECS model.

The aerodynamic model used in this work can be found in (Barros and Barros, 2017), where the wind turbine output power is calculated as follows:

$$P_T = P_w \times C_p = \frac{1}{2}\rho\pi {R_T}^2\ {v_w}^3\ C_p, \quad (4)$$

where ρ is air density (kg/m^3), R_T is the blade radius (m), and v_w is the rated wind speed (m/s). C_p represents the power coefficient of the rotor blades. Practical wind turbines have C_p in the range of 0.32 to 0.52.

The shaft model can be found in (Iov et al., 2004) and is described by:

$$T_T - T_E = J_{ech}\frac{d\,\omega_T}{dt}, \quad (5)$$

where T_T is the wind turbine mechanical torque (N.m), T_E is the PMSG electromagnetic torque (N.m) and J_{ech} is the combined turbine and generator shaft moment of inertia (Kg.m^2).

The PMSG model used in this work can be found in (Barros and Barros, 2017). The PMSG model after transformation with the power invariant Park Matrix, $T_s(\theta_r)$, for the synchronous reference frame where the d axis is aligned with the rotor flow results in:

$$v_{sd} = r_s i_{sd} + l_s\frac{d\,i_{sd}}{dt} - \omega_r l_s i_{sq}, \quad (6)$$

$$v_{sq} = r_s i_{sq} + l_s\frac{d\,i_{sq}}{dt} + \omega_r l_s i_{sd} + \sqrt{\frac{3}{2}}\omega_r\lambda_{PM}, \quad (7)$$

and

$$T_E = \sqrt{\frac{3}{2}}P\lambda_{PM}i_{sq}, \quad (8)$$

where l_s is the stator cyclic inductance and r_s is the stator resistance, $r_s = R_s$.

The MPPT strategy used in this work can be found in (Barros and Barros, 2017). The converter of PMSG is responsible for maximum power point tracking (MPPT) through ω_t control in order to respond to changes in v_w to maintain optimum operation.

Table 2: PMSG Parameters.

Parameters	Value	Unit
P	3	MW
V	690	V
ω_m	2.36	rad/s
P_p	26	-
λ_{PM}	8.53	Wb$_p$
J_m	6.758e6	Kg/m^2
L_S	0.96	mH
R_S	1.63	mΩ

2.3 Photovoltaic Generator Model

Fig. 3 depicts the simplest equivalent circuit of a solar cell as a current source in parallel with a diode, which can be found in (Villalva et al., 2009). Table 3 summarizes the PV parameters.

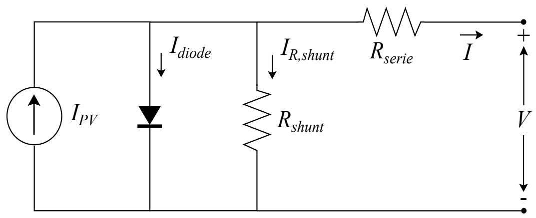

Figure 3: The equivalent circuit of a PV cell.

The output of the current source I_{PV} is directly proportional to the solar irradiation inciding on the cell. The model of the solar cell can be described by:

$$I = I_{PV} - I_{diode} - I_{R,shunt} \quad (9)$$

and

$$I = I_{PV} - I_0[e^{\frac{V+R_{serie}I}{\alpha}} - 1] - \frac{V + R_{serie}I}{R_{shunt}}, \quad (10)$$

where I_{diode} is the Shockley diode equation, I_0 is the reverse saturation or leakage current of the diode and α is the diode ideality factor.

The characteristic of the PV cell depends on external influences such as irradiation and temperature. Thus, the light-generated current of the PV cell is given by:

$$I_{PV} = (I_{PV,n} + K_I[T - T_n])\frac{G}{G_n}, \quad (11)$$

where $I_{PV,n}$ is the light-generated current at 25 $^\circ C$ and 1000 W/m^3, T is the actual temperature (Kelvin), T_n is the nominal temperature (Kelvin), G is the irradiation on the device surface (W/m^2) and G_n is the nominal irradiation (W/m^2).

The MPPT strategy used in this paper can be found in (Villalva et al., 2009). The PV array is connected usually to a switch-mode power converter, used to maintain the PV's operating at the maximum power point.

Table 3: PV parameters.

Parameters	Value	Unit
P_{PV}	244.9	W
I_{PV}	8.6503	A
N_{cell}	30	-
R_{shunt}	351.51	Ω
R_{serie}	0.38707	mΩ

2.4 Battery Energy Storage System Model

The BESS is connected to the AC grid through a converter and has nominal power of 15 MW. The BESS model is a series combination of a DC voltage source and a resistor.

The conventional grid-side control system used in this paper to control the active and reactive power supply to the AC grid can be found in (Santos and Barros, 2019).

3 Synchronverter

The synchronverter principle is to make a simple DC/AC converter to behave like a synchronous generator. The used converter is a three-phase two-level VSC with filter to reduce the voltage and current ripple caused by switching. The switching of the converter is carried out through pulse width modulation (PWM).

The model of the utilized synchronous machines can be found in (Kundur, 1994). The generated voltage, the generated reactive power, and the electromagnetic torque are given by:

$$e_{abc} = \omega M_f i_f \begin{bmatrix} \sin(\theta) \\ \sin(\theta - 2\pi/3) \\ \sin(\theta - 4\pi/3) \end{bmatrix}, \tag{12}$$

$$Q = -\omega M_f i_f \begin{bmatrix} i_a & i_b & i_c \end{bmatrix} \begin{bmatrix} \cos(\theta) \\ \cos(\theta - 2\pi/3) \\ \cos(\theta - 4\pi/3) \end{bmatrix}, \tag{13}$$

and

$$T_e = M_f i_f \begin{bmatrix} i_a & i_b & i_c \end{bmatrix} \begin{bmatrix} \sin(\theta) \\ \sin(\theta - 2\pi/3) \\ \sin(\theta - 4\pi/3) \end{bmatrix}, \tag{14}$$

where i_a, i_b, and i_c are the stator phase currents, i_f is the rotor excitation current, M_f is the mutual inductance between the field coil and each of the stator coils, and ω is the angular electric frequency.

Fig. 4 depicts the synchronverter control block diagram. The active and reactive power circuits interact through the signals e_{abc} and i_{abc}. P^* is the sum of active power references of the PV and PMSG sources and Q^* is the reactive power required by the distribution system operator (DSO).

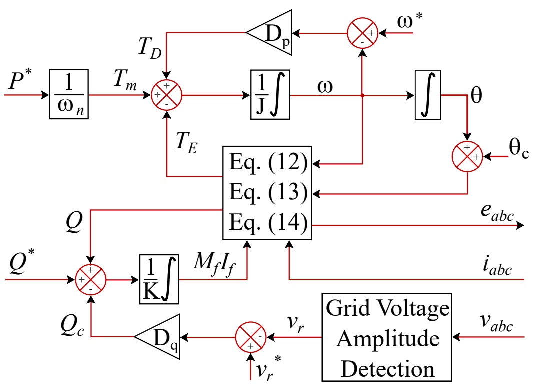

Figure 4: Synchronverter control block diagram.

where the θ_c is the angle of control for synchronization. A Phase Locked Loop (PLL) was used to synchronize the converter with the AC grid and, after system synchronization, the PLL is no longer needed for the synchronverter operation. The used PLL can be found at (Barros and Barros, 2017).

4 Simulation Results

Fig. 5 depicts the topology of the simulated microgrid, which is connected to the interconnected system through the bus 1. The converter 1 (C1) interfaces the BESS to the microgrid, the converter 2 (C2) links the eolic-photovoltaic hybrid generation system to the microgrid, and the HPP system is directly connected to the microgrid. Tables 4 and 5 depict, respectively, the VSG parameters and the parameters of the transmission lines, transformers, and loads.

Performance analyzes of the synchronverter for the microgrid operating in both the grid-connected and the island with load variations are performed. The microgrid operates in the connected mode until 1.5 second, when the islanding occurs. At 3 and 4.5 seconds, $L1$ output and input occur, respectively. These events cause microgrid frequency and voltage variations. At 6 seconds, the ICB is closed and the microgrid returns to operate in the connected mode. When the microgrid operates in connected mode, the frequency reference is imposed by the interconnected system. When the microgrid operates in island mode, the frequency reference is imposed by the HPP.

Fig. 6 depicts the active and reactive power delivered to the microgrid by the interconnected system and DG sources. The BESS delivers 12 MW and 9 MVar in both operating modes. In the connected mode, the interconnected system is responsible for energy balance of the microgrid and delivers 3 MW and 7 MVar, HPP delivers 28.4 MW and 1.6 MVAr, and eolic-photovoltaic hybrid system delivers 4 MW and 1.6 MVar. After the islanding, HPP assumes the energy balance and its active power supply decreases to 28 MW and the reactive power supply increases to 4.6 MVar. The synchronverter does not vary its active power supply due to no frequency variation, but increases its reactive power supply to 5.6 MVar due to negative voltage variation. Posteriorly, when the load output and input occurs, the HPP active power supply decreases to 19 MW and the reactive power supply decreases to 0.4 MVar. The synchronverter active power supply stays in 4 MW and the reactive power supply decreases to 1 MVar and increases to 5.6 MVar, respectively. When the microgrid returns to the connected mode, the interconnected system resumes the energy balance.

Figs. 7 and 8 depict the frequency and voltage of the synchronverter as well as its torques and reactive power. When the load output occurs, both the frequency and the voltage increase due to active and reactive excess, respectively, in the microgrid. Therefore, the synchronverter acts by decreasing the electromagnetic torque and consequently the active power supply and by decreasing reactive power supply, while HPP starts to act by reducing its energy supply to microgrid. When the

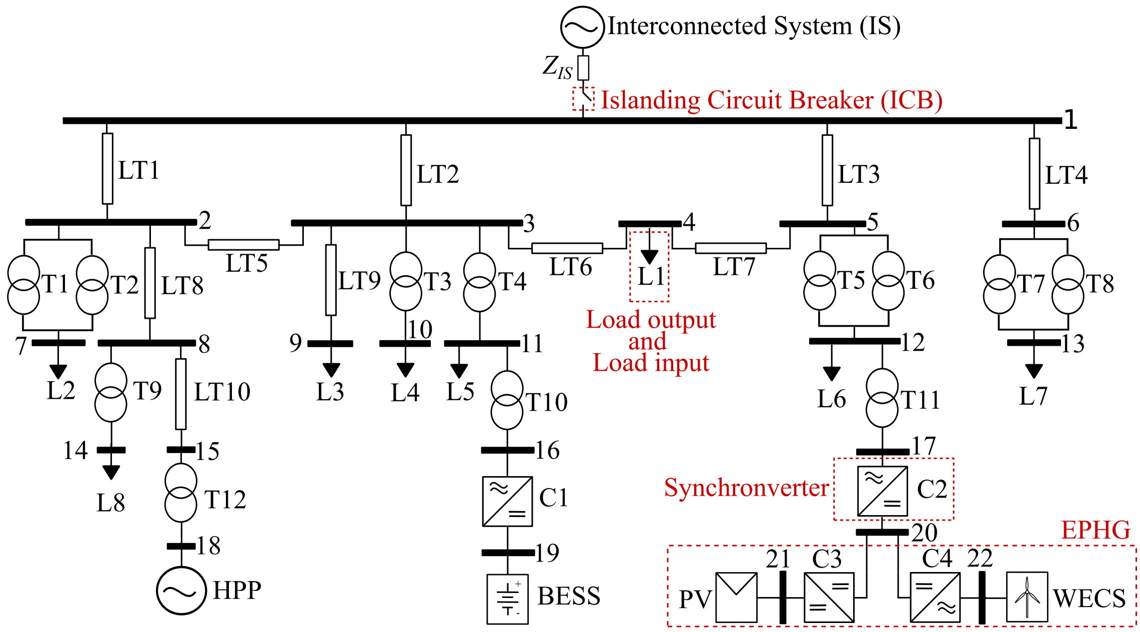

Figure 5: Microgrid configuration.

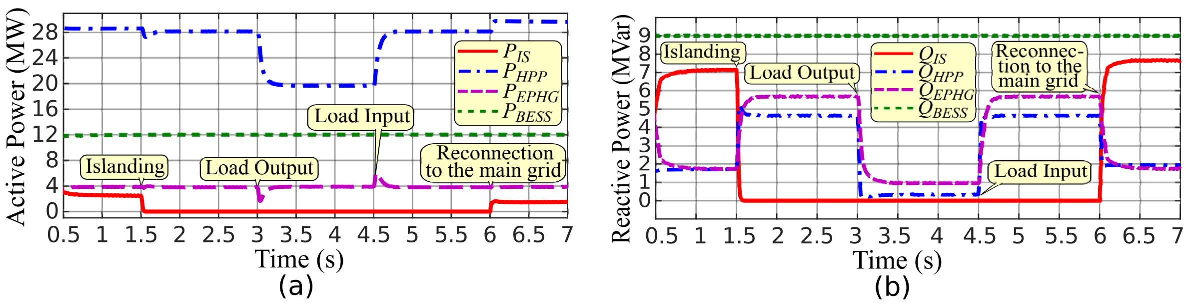

Figure 6: Power flows delivered of the interconnected system and DG sources to the microgrid: (a) active power; (b) reactive power.

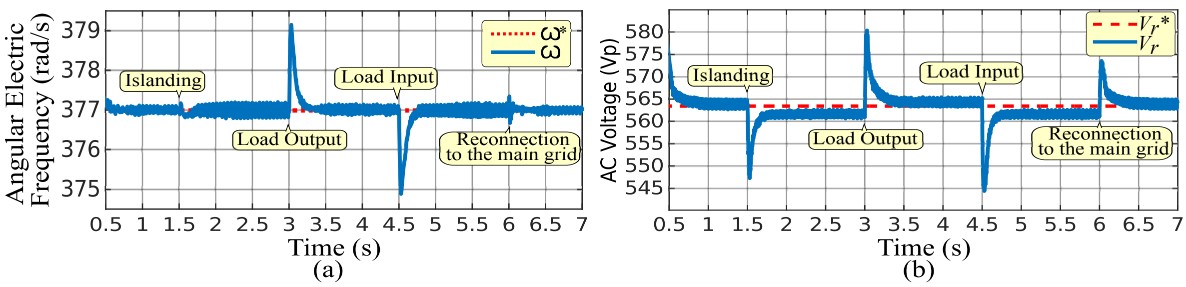

Figure 7: Control variables of the synchronveter: (a) angular electric frequency; (b) voltage amplitude.

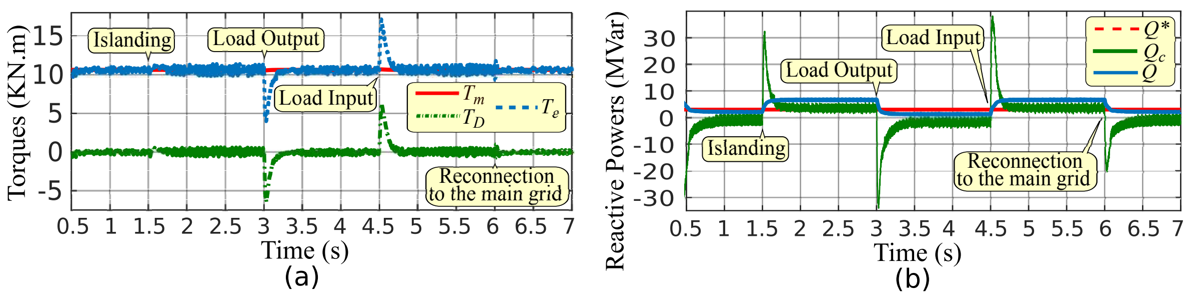

Figure 8: Acting variables of the synchronveter: (a) torques; (b) reactive powers.

load input occurs, the frequency and AC voltage of the microgrid decrease due to power shortage. Therefore, the synchronverter increases active and reactive power supply, while HPP acts by increasing the power supply. The synchronverter, having a faster response than HPP, provides frequency and voltage support, while HPP maintains the energy balance of the microgrid.

Table 4: VSG parameters.

Parameters	Value	Unit
ω^*	377	rad/s
V^*	563	V
Q^*	2	MVar
D_p	2100	-
J	4.2	-
D_q	100e4	-
K	7.54e5	-

Table 5: Transmission lines, transformers, and loads parameters.

	R (Ω)	X (Ω)	C (nF)	P (MW)	Q ($MVar$)
$LT1$	6.570	28.83	632.9	-	-
$LT2$	16.96	24.98	416.8	-	-
$LT3$	5.110	12.40	253.5	-	-
$LT4$	0.015	11.92	198.9	-	-
$LT5$	8.094	11.92	198.9	-	-
$LT6$	2.680	6.503	132.6	-	-
$LT7$	2.204	5.351	109.2	-	-
$LT8$	4.894	12.83	232.3	-	-
$LT9$	2.620	6.360	129.8	-	-
$LT10$	1.104	1.625	27.30	-	-
$T1$	-	68.75	-	-	-
$T2$	-	36.14	-	-	-
$T3$	-	59.99	-	-	-
$T4$	-	61.32	-	-	-
$T5$	-	66.59	-	-	-
$T6$	-	35.09	-	-	-
$T7$	-	36.04	-	-	-
$T8$	-	36.04	-	-	-
$T9$	-	60.37	-	-	-
$T10$	-	6.540	-	-	-
$T11$	-	1.270	-	-	-
$T12$	-	60.37	-	-	-
$L1$	-	-	-	10.9	4.34
$L2$	-	-	-	6.35	2.51
$L3$	-	-	-	1.13	0.31
$L4$	-	-	-	1.83	0.19
$L5$	-	-	-	1.78	0.95
$L6$	-	-	-	7.00	2.10
$L7$	-	-	-	8.33	4.79
$L8$	-	-	-	1.72	1.02

5 Conclusions

This paper presented the performance evaluation in frequency and voltage support of the eolic-photovoltaic hybrid generation system connected to the microgrid through the converter controlled by virtual synchronous generator technique of synchronverter. The microgrid can operate in the grid-connected and the island with load variation modes.

The synchronverter operating in the microgrid provided a good performance because it presented a faster response to transients in the grid than hydro power plants, providing frequency and voltage support, while hydro power plant maintained the energy balance of microgrid. Therefore, the system had a high reliability in terms of stability. Besides, renewable energy sources equipped with the synchronverter do not demand reactive power from the grid.

Acknowledgment

This work was supported by the National Council for Scientic and Technological (CNPq) and by the Coordination for the Improvement of Higher Education Personnel (CAPES), Brazil.

References

Barros, L. S. and Barros, C. M. V. (2017). An internal model control for enhanced grid-connection of direct-driven pmsg-based wind generators., *Electric Power Systems Research* pp. 440–450.

Iov, F., Hansen, A., Sorensen, P. and Blaabjerg., F. (2004). *Wind Turbine Blockset in MATLAB/Simulink.*, Aalborg University.

Kersting., W. H. (2002). *Distriution System Modeling and Analysis.*, CRC press LLC.

Kundur, P. (1994). *Power System Stability and Control.*, Mc. Graw Hill.

Meng, L., Savaghebi, M., Andrade, F., Vasquez, J. C., Guerrero, J. M. and Graells, M. (2015). Microgrid central controller development and hierarchical control implementation in the intelligent microgrid lab of aalborg university., *Proc. IEEE Appl. Power Electron. Conf. Expo. (APEC)* pp. 2585–2592.

Mercier, P., Cherkaoui, R. and Oudalov, A. (2009). Optimizing a battery energy storage system for frequency control application in an isolated power system., *IEEE Trans. Power Syst.* pp. 1469–1477.

Santos, M. S. and Barros, L. S. (2019). Offshore wind energy conversion system based on squirrel cage induction generator connected to the grid by vsc-hvdc link., *Innovative Smart Grid Technologies Conference - Latin America (ISGT LA)* pp. 15–18.

Villalva, M., Gazoli, J. R. and Filho, E. R. (2009). Comprehensive approach to modeling and simulation of photovoltaic array., *IEEE Trans on Power Electronics* pp. 1198–1208.

Zhong, Q. and Rohner, G. W. (2011). Microgrid central controller development and hierarchical control implementation in the intelligent microgrid lab of aalborg university., *Synchronverters: Inverters That Mimic Synchronous Generators.* pp. 1259–1267.